Dynamics in carbon exchange fluxes for a grazed semi-arid savanna ecosystem in West Africa

Tagesson, Torbern; Fensholt, Rasmus; Cropley, Ford; Guiro, Idrissa; Horion, Stephanie; Ehammer, Andrea; Ardö, Jonas

Published in:
Agriculture, Ecosystems & Environment

DOI:
10.1016/j.agee.2015.02.017

2015

Document Version:
Publisher's PDF, also known as Version of record

Agriculture, Ecosystems and Environment 205 (2015) 15–24

Contents lists available at ScienceDirect

Agriculture, Ecosystems and Environment

journal homepage: www.elsevier.com/locate/agee

Dynamics in carbon exchange fluxes for a grazed semi-arid savanna ecosystem in West Africa

Torbern Tagesson [a,*], Rasmus Fensholt [a], Ford Cropley [c], Idrissa Guiro [b], Stéphanie Horion [a], Andrea Ehammer [a], Jonas Ardö [c]

[a] Department of Geosciences and Natural Resource Management, University of Copenhagen, Øster Voldgade 10, DK-1350 Copenhagen, Denmark
[b] Laboratoire d'Enseignement et de Recherche en Géomatique, Ecole Supérieure Polytechnique, Université Cheikh Anta Diop de Dakar, BP 25275 Dakar-Fann, Senegal
[c] Department of Physical Geography and Ecosystem Science, Lund University, Sölvegatan 12, SE-223 62 Lund, Sweden

ARTICLE INFO

Article history:
Received 3 September 2014
Received in revised form 26 February 2015
Accepted 28 February 2015
Available online xxx

Keywords:
Net ecosystem exchange
Gross primary productivity
Sahel
Regression tree
Light use efficiency

ABSTRACT

The main aim of this paper is to study land–atmosphere exchange of carbon dioxide (CO_2) for semi-arid savanna ecosystems of the Sahel region and its response to climatic and environmental change. A subsidiary aim is to study and quantify the seasonal dynamics in light use efficiency (ε) being a key variable in scaling carbon fluxes from ground observations using earth observation data. The net ecosystem exchange of carbon dioxide (NEE) 2010–2013 was measured using the eddy covariance technique at a grazed semi-arid savanna site in Senegal, West Africa. Night-time NEE was not related to temperature, confirming that care should be taken before applying temperature response curves for hot dry semi-arid regions when partitioning NEE into gross primary productivity (GPP) and ecosystem respiration (R_{eco}). Partitioning was instead done using light response curves. The values of ε ranged between 0.02 g carbon (C) MJ^{-1} for the dry season and 2.27 g C MJ^{-1} for the peak of the rainy season, and its seasonal dynamics was governed by vegetation phenology, photosynthetically active radiation, soil moisture and vapor pressure deficit (VPD). The CO_2 exchange fluxes were very high in comparison to other semi-arid savanna sites; half-hourly GPP and R_{eco} peaked at -43 μmol CO_2 m^{-2} s^{-1} and 20 μmol CO_2 m^{-2} s^{-1}, and daily GPP and R_{eco} peaked at -15 g C m^{-2} and 12 g C m^{-2}, respectively. Possible explanations for the high CO_2 fluxes are a high fraction of C4 species, alleviated water stress conditions, and a strong grazing pressure that results in compensatory growth and fertilization effects. We also conclude that vegetation phenology, soil moisture, radiation, VPD and temperature were major components in determining the seasonal dynamics of CO_2 fluxes. Despite the height of the peak of the growing season CO_2 fluxes, the annual C budget (average NEE: -271 g C m^{-2}) were similar to that in other semi-arid ecosystems because the short rainy season resulted in a short growing season. Global circulation models project a decrease in rainfall, an increase in temperature and a shorter growing season for the western Sahel region, and the productivity and the sink function of this semi-arid ecosystem may thus be lower in the future.

1. Introduction

The African Sahel region is located south of the Sahara desert and the area is dominated by semi-arid grassland with shrubs and low tree coverage. The region is strongly dependent on rain-fed agriculture and pastoral livelihood, and drought and famine frequently impact the people living in the region (OECD, 2009). The semi-arid ecosystems in the Sahel are vulnerable to the effects of climate change, because of this rainfall dependency (e.g. Hickler et al., 2005). Climate thereby strongly affects the land-atmosphere carbon dioxide (CO_2) exchange processes which can have strong positive or negative feedbacks on the climate system. Recently, it has been shown that semi-arid ecosystems has an increasingly important function as a sink of the global carbon cycle, because of increased rainfall and CO_2 fertilization effects (Donohue et al., 2013). In the future, semi-arid regions can even overrule tropical forests in dominance affecting the inter-annual variability in the global carbon cycle (Poulter et al., 2014).

* Corresponding author. Tel.: +46 704 99 39 36; fax: +45 35 32 25 01.
E-mail addresses: torbern.tagesson@ign.ku.dk (T. Tagesson), rf@ign.ku.dk (R. Fensholt), ford.cropley@nateko.lu.se (F. Cropley), idyguiro@yahoo.fr (I. Guiro), stephanie.horion@ign.ku.dk (S. Horion), andrea.ehammer@ign.ku.dk (A. Ehammer), jonas.ardo@nateko.lu.se (J. Ardö).

http://dx.doi.org/10.1016/j.agee.2015.02.017
0167-8809/

It is thereby important to study variability in the land atmosphere CO_2 exchange processes for semi-arid savanna regions. The net ecosystem exchange of CO_2 (NEE) is the balance between the CO_2 assimilated through gross primary production (GPP) by the vegetation and the carbon (C) decomposed and released as CO_2 by ecosystem respiration (R_{eco}). There have only been a few studies investigating temporal dynamics of the CO_2 exchange processes using the eddy covariance technique in the Sahel region, and most of them only cover a few weeks of data (e.g. Verhoef et al., 1996; Friborg et al., 1997; Moncrieff et al., 1997b; Hanan et al., 1998; Ardö et al., 2008). To our knowledge there are only three previous studies of land atmosphere exchange of CO_2 based on EC data from the Sahel region which covered an inter-annual period (Boulain et al., 2009; Merbold et al., 2009; Tagesson et al., 2015). However, none of these studies has focused on the temporal dynamics in the CO_2 exchange processes and their budgets. The CO_2 exchange processes are known to vary considerably and many controlling factors for these variations have been suggested: temperature, radiation regime, species composition, and moisture and nutrient availability (Lloyd and Taylor, 1994; Semmartin and Oesterheld, 1996; Rockström and de Rouw, 1997; Chapin et al., 2002; Hanan et al., 2011).

Due to the lack of in situ measurements, earth observation has proved an important tool in studying the ecosystem properties of the Sahel. Within earth observation, it is common to estimate GPP using a light use efficiency (LUE) model (Monteith, 1972, 1977). The LUE-model calculates GPP from the photosynthetically active radiation absorbed by the vegetation (APAR), using a simple conversion efficiency coefficient (the light use efficiency, ε). Initially, ε was considered to be relatively constant, but substantial differences have been found between plant communities, and also due to species composition, development stage, and stress level (Goetz and Prince, 1996; Gower et al., 1999; Drolet et al., 2008). Values of ε and its constraining factors therefore need to be investigated for various plant communities when GPP is to be estimated over larger areas. The main aim of this paper is to make a detailed study of the CO_2 exchange processes of a semi-arid savanna ecosystem in the Sahel region, and their response to climatic and environmental change. Our long time series of CO_2 fluxes allowed us to study the seasonal and diurnal variation in CO_2 fluxes and the influence of hydro-climatic variables (air and soil temperature, relative air humidity, photosynthetically active radiation (PAR), vapor pressure deficit (VPD), rainfall and soil moisture) and vegetation phenology. In addition, our CO_2 flux measurements allow us to estimate annual C budgets for the land-atmosphere exchange processes, and to study inter-annual variation of these budgets. A final objective was to quantify and study the seasonal dynamics of ε to better understand the temporal variability in ε to be implemented in improved earth observation based productivity models.

2. Material and methods

2.1. Site description

The measurements were conducted north-east of the town of Dahra in the Ferlo region of Senegal, West Africa (15.40 °N, 15.43 °W, elevation 40 m). The Dahra measurement site is located in the Sahelian ecoclimatic zone. Annual mean rainfall is 416 mm (for the period 1951–2003) of which more than 95% of the rain falls during the rainy season (July–October), with August being the wettest month (Agence Nationale de l'Aviation Civile et de la Météorologie, Senegal). Annual air temperature (period 1951–2003) is 29 °C; May has the highest mean monthly temperature (32 °C) and January the lowest (25 °C). South-westerly winds dominate during the rainy season, whereas north-easterly winds dominate during the dry season. The leaf area index (LAI) generally ranges between 0 and 2 (Fensholt et al., 2004). The growing season closely follows the rainy season and is short (2–3 months). The site is a typical low tree and shrub savanna environment with ~3% tree cover (Rasmussen et al., 2011). The most abundant tree species are *Balanites aegyptiaca*, *Acacia tortilis* and *Acacia Senegal*. The species composition of the ground vegetation for the years 2010–2013 is given in Table 1 (Mbow et al., 2013; Tagesson et al., 2015). The study area is homogenous and flat, and the dominant plant communities extend for several kilometers in all directions surrounding the study site. The soil is sandy luvic arenosol with low amounts of organic material and low clay content (clay = 0.35%, silt = 4.61%, and sand = 95.04%). The land is grazed and located within the Centre de Recherches Zootechniques de Dahra of the Institut Sénégalais de Recherche Agricole (ISRA). For a complete description of the site and the measurements conducted at Dahra, see Tagesson et al., 2015.

2.2. Eddy covariance measurements

The NEE (μmol $CO_2\,m^{-2}\,s^{-1}$) measurements were done between 8 August 2010 and 31 December 2013 using an EC system which had a 3-axis Gill R3 Ultrasonic Anemometer (GILL instruments UK) and an open-path CO_2/H_2O infrared gas analyzer (LI-7500, LI-COR Inc. Lincoln, Nebraska, USA) installed at 9 m height. The open-path analyzer was tilted 29° from vertical with 20 cm northward separation and −24 cm vertical separation from the anemometer. The anemometer and infrared gas analyzer data were sampled at 20 Hz. Every 4 weeks, the span and the offset of the gas analyzer were measured and the gas analyzer was calibrated. We processed the raw EC data using EddyPro 4.2.1 software (LI-COR Biosciences, 2012), and the fluxes were calculated for 30 min periods. The processing includes despiking (Vickers and Mahrt, 1997) (plausibility range: window average ±3.5 standard deviations), 2-D coordinate rotation (Wilczak et al., 2001), time lag removal between anemometer and gas analyzer by covariance maximization

Table 1
Dominant species of the herbaceous vegetation at the Dahra field site in 2010–2013. For a complete list of species composition, see Supplementary material of Tagesson et al., 2015

	2010	2011	2012	2013
Dominant species	Aristida adscensionis	Aristida adscensionis	Aristida adscensionis	Aristida mutabilis
	Zornia latifolia	Dactyloctenium aegypticum	Cenchrus biflorus	Eragrostis tremula
	Cenchrus biflorus	Zornia latifolia	Dactyloctenium aegypticum	Zornia glochidiata
	Dactyloctenium aegypticum	Eragrostis tremula	Zornia latifolia	Dactylotenium aegyptium
	Eragrostis tremula	Cenchrus biflorus	Eragrostis tremula	Alysicarpus ovalifolius

(Fan et al., 1990), linear detrending (Moncrieff et al., 2004), and compensation for density fluctuations (Webb et al., 1980). The fluxes were corrected for low and high pass filtering effects (Moncrieff et al., 2004, 1997a). The data were filtered according statistical tests as recommended by Vickers and Mahrt (1997), and for steady state conditions and for fully developed turbulent conditions following Foken et al. (2004). Measurements made during heavy rainfall were also filtered out; 44% of the combined sonic anemometer and gas analyzer data were filtered out, but in total, there were 73% gaps in the data. The reasons for the large amount of missing data were minor breaks due to power failure, large gaps caused by broken sensors from 5 November 2010–17 July 2011 and 11 January 2013–7 July 2013, and that more than 40% is commonly filtered out for open path sensors (e.g. Tagesson et al., 2012b). The main parts of the growing seasons 2010–2013 were covered, whereas the large data gaps are mainly located during the dry seasons without much vegetation activity.

2.3. Measurements of environmental variables

Meteorological and hydrological variables were measured during the entire study period, except for 26 October 2010–25 February 2011 (technical issues). The measured variables were air temperature (°C), relative air humidity (%), incoming ($_{inc}$) and reflected ($_{ref}$) PAR (μmol photons $m^{-2}\,s^{-1}$), PAR transmitted through the vegetation ($PAR_{transmit}$), incoming and reflected red and near infrared (NIR) radiation (MODIS red/NIR spectral configuration) (μmol $m^{-2}\,s^{-1}$), rainfall (mm), soil temperature (°C), and soil moisture (%) (Table 2). All sensors were connected to a CR-1000 logger in combination with a multiplexer (Campbell Scientific Inc. North Logan, USA). Data were sampled every 30 s and stored as 15 min averages (sum for rainfall).

The incoming and reflected red and NIR radiation measurements were used to estimate the NDVI as:

$$NDVI = \frac{(\rho_{NIR} - \rho_{red})}{(\rho_{NIR} + \rho_{red})} \quad (1)$$

where ρ_{NIR} and ρ_{red} are the hemispherical reflectance in the red and NIR bands respectively.

The PAR absorbed by the vegetation (APAR) was estimated by:

$$APAR = PAR_{inc} - PAR_{ref} - (1 - \alpha_{soil}) \times PAR_{transmit} \quad (2)$$

where α_{soil} is the albedo of the soil, which was measured as 0.20 (Tagesson et al., 2015).

The total above ground herbaceous biomass (g m^{-2}) was sampled approximately every 10 days during the rainy seasons at 28 one m^2 plots located along two ~1060 m long transects (Mbow et al., 2013). The method applied was destructive, so even though the same transects were used for each sampling date, the plots were never located at exactly the same location. All above ground green vegetation matter was collected and weighed in the field to get the fresh weight. The dry matter (DW) was estimated by oven-drying the green biomass. For a thorough description regarding the biomass sampling we refer to Mbow et al. (2013). The DW was then converted to g C m^{-2} using a conversion factor of 0.5 (Schlesinger, 1997). For estimating total herbaceous biomass, we assumed that root biomass was 60% of above ground biomass (Wilsey and Wayne, 2006).

2.4. Environmental controls on short-term variation in daytime and night-time NEE

To study environmental controls on diurnal variability in the CO_2 fluxes, the half-hourly NEE data were separated into daytime (solar radiation >20 W m^{-2}) and night-time data. Daytime NEE is the sum of GPP and R_{eco}. There is no photosynthetic activity during night-time, when NEE is simply equal to R_{eco}. We used a 7-day moving window with a 1 day time step to analyze environmental controls on the half-hourly fluxes, by fitting ordinary least-square linear and exponential regressions for each 7-day moving window. In this way, we analyzed the relationships between daytime NEE and soil moisture (at all depths), relative air humidity, air temperature, and VPD (kPa). The effect of PAR_{inc} on daytime-NEE was estimated using the non-linear Misterlich light-response function:

$$NEE = -(F_{csat} + R_d) \times \left(1 - e^{\left(\frac{-\alpha \times PAR}{F_{csat} + R_d}\right)}\right) + R_d \quad (3)$$

where F_{csat} is the CO_2 uptake at light saturation, R_d is dark respiration and α is the quantum efficiency (μmol CO_2

Table 2
Basic information regarding the measured environmental variables. PAR is photosynthetically active radiation, inc is incoming, ref is reflected, and NIR is near infrared. The red and NIR radiation was measured using the same spectral configuration as that of the MODIS sensor.

Variable	Measurement height (m)	Sensor	Company
Air temperature (°C)	2	Campbell CS215	Campbell Scientific Inc., North Logan, USA
Relative air humidity (%)	2	Campbell CS215	Campbell Scientific Inc., North Logan, USA
PAR_{inc} (μmol $m^{-2}\,s^{-1}$)	10.5	Quantum SKP 215 sensor	Skye instruments Ltd., Llandridod wells, UK
PAR_{ref} (μmol $m^{-2}\,s^{-1}$)	10.5	Quantum SKP 215 sensor	Skye instruments Ltd., Llandridod wells, UK
$PAR_{transmit}$ (μmol $m^{-2}\,s^{-1}$)	0.01	6 Quantum SKP 215 sensor	Skye instruments Ltd., Llandridod wells, UK
Red_{inc} (centered at 650 nm, bandwidth 40 nm) (μmol $m^{-2}\,s^{-1}$)	10.5	Hemispherical two-channel SKR 1800 sensor	Skye instruments Ltd., Llandridod wells, UK
Red_{ref} (centered at 650 nm, bandwidth 40 nm) (μmol $m^{-2}\,s^{-1}$)	10.5	Hemispherical two-channel SKR 1800 sensor	Skye instruments Ltd., Llandridod wells, UK
NIR_{inc} (centered at 860 nm, bandwidth 40 nm) (μmol $m^{-2}\,s^{-1}$)	10.5	Hemispherical two-channel SKR 1800 sensor	Skye instruments Ltd., Llandridod wells, UK
NIR_{ref} (centered at 860 nm, bandwidth 40 nm) (μmol $m^{-2}\,s^{-1}$)	10.5	Hemispherical two-channel SKR 1800 sensor	Skye instruments Ltd., Llandridod wells, UK
Rainfall (mm)	2	4 ARG1000 rain gauges	Waterra, Burnaby, Canada
Soil temperature (°C)	−0.05, −0.1, −0.5	Campbell 107 temperature probe	Campbell Scientific Inc., North Logan, USA
Soil moisture (%)	−0.05, −0.1,−0.3, −0.5, −1.0	HH2 Delta probe	Delta T devices, Cambridge UK

μmol PAR^{-1}) or the initial slope of the light response curve (Falge et al., 2001).

Ordinary least-square linear and exponential regressions were also fitted between night-time NEE and soil moisture at all measured depths, and versus relative air humidity for each 7-day period. Ecosystem respiration is generally considered to follow an exponential relationship with temperature, and the Lloyd and Taylor (1994) equation was developed to estimate R_{eco} for several different ecosystem types:

$$R_{eco} = R_{10} \times e^{\left(\frac{1}{56.02} - \frac{1}{T+273.15-227.13}\right)} \quad (4)$$

where R_{10} is the respiration rate at 10 °C, and T is the air and soil temperature (°C). We fitted Eq. (4) with night-time NEE against air temperature, and soil temperature at all measured depths for each 7-day moving window.

2.5. Gap filling and partitioning of net ecosystem exchange between gross primary productivity and ecosystem respiration

To determine daytime R_{eco}, it is common to parameterize exponential functions (Eq. (4)) between night-time NEE and soil temperature, and to apply these during daytime (Reichstein et al., 2005). However, it has been reported that care should be taken before applying these relationships to hot dry semi-arid savanna ecosystems (Archibald et al., 2009). For the 7-day moving windows, we did not find any relationship between night-time NEE, and any of the measured variables. Instead, we thereby partitioned daytime NEE between GPP and R_{eco} using the Misterlich light response function (Eq. (3)) against PAR_{inc} (Falge et al., 2001). To account for VPD limits on GPP, the fixed F_{csat} parameter in Eq. (3) was replaced with an exponential decreasing function:

$$F_{csat} = \begin{cases} F_{csat}, e^{-k(VPD-VDP_0)} & VPD > VPD_0 \\ F_{csat} & VPD < VPD_0 \end{cases} \quad (5)$$

where VPD_0 is 10 hPa following the method by Lasslop et al. (2010). Eq. (3) in combination with Eq. (5) was parameterized for daytime NEE using the same 7-day moving windows as in the Section 2.4. By subtracting R_d the function was forced through 0, and GPP was thereby estimated:

$$GPP = -(F_{csat} + R_d) \times \left(1 - e^{\left(\frac{-\alpha \times PAR}{F_{csat}+R_d}\right)}\right) \quad (6)$$

Ecosystem respiration was calculated by subtracting modeled GPP from measured NEE.

Gaps in NEE and GPP shorter than or equal to 3 days were filled in one of four different ways: (i) linear interpolation were used for gaps shorter than 2 h (Falge et al., 2001); (ii) the Misterlich light-response function (Eqs. (3) and (5) (NEE) and (6) and (5) (GPP)) for the 7-day moving windows were used for daytime gaps longer than 2 h (Falge et al., 2001); (iii) night-time gaps were filled using average NEE measured during that night; (iv) any remaining gaps were filled using mean diurnal variation calculated for the 7-days moving windows (Falge et al., 2001). Finally, R_{eco} was gap filled by subtracting gap-filled GPP from gap-filled NEE.

2.6. The light use efficiency

The LUE-model is a linear function between GPP and APAR:

$$GPP = \varepsilon \times APAR \quad (7)$$

The validity of this function requires a reasonably linear relationship between assimilated CO_2 and APAR (Fig. 1). To estimate the seasonal dynamics of ε (μmol CO_2 μmol APAR^{-1}), linear regressions were fitted with NEE_{day} against APAR for the 7-day moving window. The ε values were later converted to g C MJ APAR^{-1}. Just to clarify the difference between quantum efficiency (α) and light use efficiency (ε); α is the initial slope of Eq. (3) against PAR_{inc}, whereas ε is the slope of a linear curve against APAR.

2.7. Seasonal dynamics in carbon fluxes and light-use efficiency

To study how well environmental variables determine the seasonal dynamics in NEE, GPP, R_{eco} and ε, we used regression tree analysis. It is a robust statistical tool to analyze complex, nonlinear relationships and interactions between a single response variable and several explanatory variables (De'ath and Fabricius, 2000). The data set is repeatedly split into more and more homogeneous subgroups, each categorized by values of both the dependent and the independent variables. Splitting continues until a tree is created, which is then pruned back to a proper size according a cross validation procedure. We required at least five days in each subgroup to allow further splitting of the tree. In each analysis, we separated the data into ten subgroups of approximately equal size. Each subgroup was left out once, and ten trees were created with the remaining nine subgroups, which were evaluated against the left-out subgroup. The error was summed for all ten trees and for each of the different tree sizes. The smallest tree with the minimum error was selected. The cross-validation was repeated 100 times and the most common tree size was used in the final analysis. For a more detailed description of tree regression analysis and its advantages, see De'ath and Fabricius (2000).

As explanatory variables for daily sums of NEE, we used NDVI, PAR, air temperature, VPD, soil temperature and soil moisture (0.05 m depth). As explanatory variables for daily sums of GPP and ε, we used NDVI, PAR, air temperature, VPD, soil temperature, and soil moisture (0.05 m depth). In the flux partitioning, R_{eco} was estimated as the difference between NEE and GPP and a regression between R_{eco} and GPP would thereby result in a false correlation, as the variables are not independent. In order to include daily sums of GPP as an explanatory variable for R_{eco}, we used the average night-time R_{eco} estimates as an independent variable in the R_{eco} regression tree analysis. As explanatory variables, we used daily sums of GPP, NDVI, air temperature, VPD, and soil temperature and soil moisture (0.05 m depth).

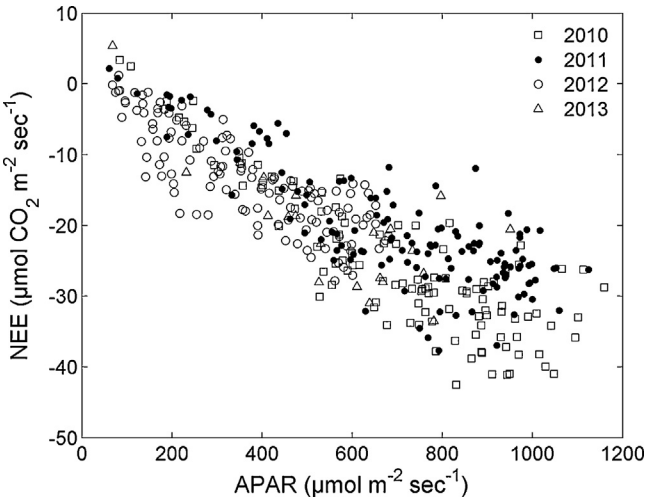

Fig. 1. Daytime net ecosystem exchange (NEE) against absorbed photosynthetic active radiation (APAR) for the 7-day period at the peak of the growing season 2010–2013.

2.8. The annual C flux budgets

For calculating the C flux budgets for 2010 to 2013, it was necessary to fill gaps in NEE, GPP and R_{eco} longer than three days, which was done using regression trees. We choose 100 tree sizes by running 100 series of cross validation (De'ath and Fabricius, 2000). For each series, the tree with the minimum error was chosen and used for predicting the CO_2 fluxes. The 100 CO_2 flux subsets were then averaged. For the period without environmental variables, when the regression trees could not be applied, we used the CO_2 fluxes from the same DOY the year after. The total annual C budgets were calculated by summing all NEE, GPP and R_{eco} fluxes for the years 2010–2013.

The uncertainty in the C flux budgets caused by random error (E_{rand}) was estimated following the method by Finkelstein and Sims (2001), whereas systematic errors were estimated following the method by Aurela et al. (2002) (Appendix A). All errors were added together using the error accumulation principle:

$$E_{tot} = \sqrt{{E_{rand}}^2 + {E_{gf}}^2 + {E_{filt}}^2 + {E_{freq}}^2} \quad (8)$$

where E_{tot} is the total accumulated error, E_{gf} is the errors from the gap filling, E_{filt} is the error associated with thresholds for the filtering of the data, and E_{freq} is the errors caused by frequency corrections.

3. Results

3.1. Diurnal variation in the CO_2 fluxes

The diurnal peak of GPP was slightly before the peak of the incoming radiation, which is at 13:00, and GPP was slightly higher in the morning than in the afternoon (Fig. 2). Ecosystem respiration was low and high during night-time and daytime, respectively. There were no relationships between night-time half-hourly NEE and any of the measured environmental variables (air temperature, VPD, soil moisture or soil temperature at any depth) for the 7-day periods. No clear seasonality in the correlations could be seen indicating that during no specific period over the season were any of these factors in control of the night-time half-hourly NEE. The same outcome was obtained whether the fitted regression function was linear or exponential.

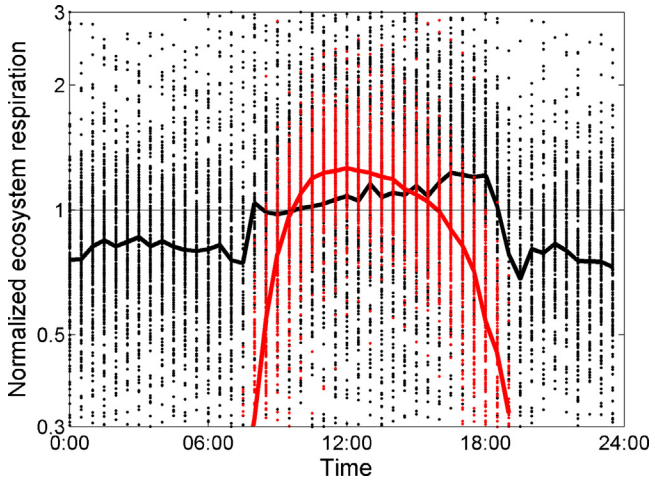

Fig. 2. Diurnal variation in ecosystem respiration (R_{eco}; black) and gross primary productivity (GPP; red). The half-hourly flux estimates were normalized by dividing each half-hourly value by the mean daily flux. We only used data from days with more than 70% data coverage (in total 305 days). The thick lines are the median normalized fluxes and the dots are each half-hour value. (For interpretation of the references to color in this figure legend, the reader is referred to the web version of this article.)

For the 7-day periods, there were no correlations between daytime half-hourly NEE and air temperature, VPD, soil moisture or soil temperature at any depth. There was however a strong relationship between daytime half-hourly NEE and PAR, following the Misterlich light-response function, for all periods except for DOY 158 and DOY 177-179 2012 (average $R^2 = 0.55$). DOY 158 was during the end of the dry season, when productivity was low. The period DOY 177-179, 2012 is at the beginning of the rainy season, when there was a large burst in R_{eco} (Fig. 3d). This positive flux in CO_2 masked the low productivity, explaining the lack of relationship at this time.

3.2. Seasonal dynamics in CO_2 fluxes and light use efficiency

The highest and lowest CO_2 fluxes were measured during the rainy season 2010, and the dry period 2012, respectively (Fig. 3d). R_{eco} dominated the NEE at the start of the rainy season, resulting in strong release of CO_2. The sink function was strong during the peak of the growing season, with daily peak NEE of $\sim -7.5\,g\,C\,m^{-2}$. The daily GPP and R_{eco} peaked at $\sim -15\,g\,C\,m^{-2}$ and $\sim 12\,g\,C\,m^{-2}$, respectively. Fluxes decreased strongly towards the end of the rainy season.

There were strong seasonal variations in the parameters estimated by the Misterlich function (Fig. 3e and f). The α ranged between $0.006\,g\,C\,MJ\,PAR^{-1}$ for the dry season in 2012, to $1.38\,g\,C\,MJ\,PAR^{-1}$ for the peak of the growing season 2013. The saturation level of GPP that were within a realistic range were between 0.2 and 57.0 mg $CO_2\,m^{-2}\,h^{-1}$, corresponding to the dry season 2012 and the rainy season 2010, respectively. Occasionally, during the dry seasons, the relationships were very linear, resulting in infinite saturation levels (the vertical lines in Fig. 3e). There was also strong seasonal variation in ε, which ranged between $0.02\,g\,C\,MJ\,APAR^{-1}$ and $2.27\,g\,C\,MJ\,APAR^{-1}$ corresponding to the dry and rainy seasons, respectively (Fig. 3f).

In the regression tree analysis, all variables used as input data were repeated observations of the same measurement plot. The variables cannot therefore be regarded as statistically independent; they are temporally auto-correlated, and it is therefore hard to tell exactly which explanatory variable controls the CO_2 fluxes. The regression tree analyses do however indicate which variables best determined the CO_2 fluxes. The variables determining seasonal variation in NEE were NDVI, PAR, soil moisture, and VPD, in that order (pruning level = 16, $R^2 = 0.70$). The variables determining the seasonal variation in GPP were NDVI, soil moisture, VPD, PAR, and air temperature (pruning level = 24, $R^2 = 0.93$). The variables determining the seasonal variation in daily R_{eco} were NDVI, soil moisture, GPP, VPD and soil temperature, (pruning level = 20, $R^2 = 0.86$). Finally, the environmental variables determining the seasonal dynamics in ε were NDVI, soil moisture, VPD, PAR, and air temperature (pruning level = 25, $R^2 = 0.54$).

3.3. The annual C flux budgets

The site acted as a C sink for all three years with an average ($\pm$ 1 standard error) annual total NEE of $-271 \pm 39\,g\,C\,m^{-2}\,y^{-1}$ (Table 3). Total herbaceous biomass and annual NEE budgets are in the same order, even though the NEE budget was slightly higher for 2010, and slightly lower for 2011–2013 (Table 3). The average annual sums of GPP and R_{eco} were $-1076 \pm 46\,g\,C\,m^{-2}\,y^{-1}$ and $772 \pm 87\,g\,C\,m^{-2}\,y^{-1}$, respectively (Fig. 4), with slight inter-annual variation. The annual sums of R_{eco} was significantly (p-value >0.05) correlated with air temperature ($r = -0.98$), rainfall ($r = 0.98$), and start of rainy season ($r = -0.98$). There was no significant correlations for the annuals sums of GPP but it was closely

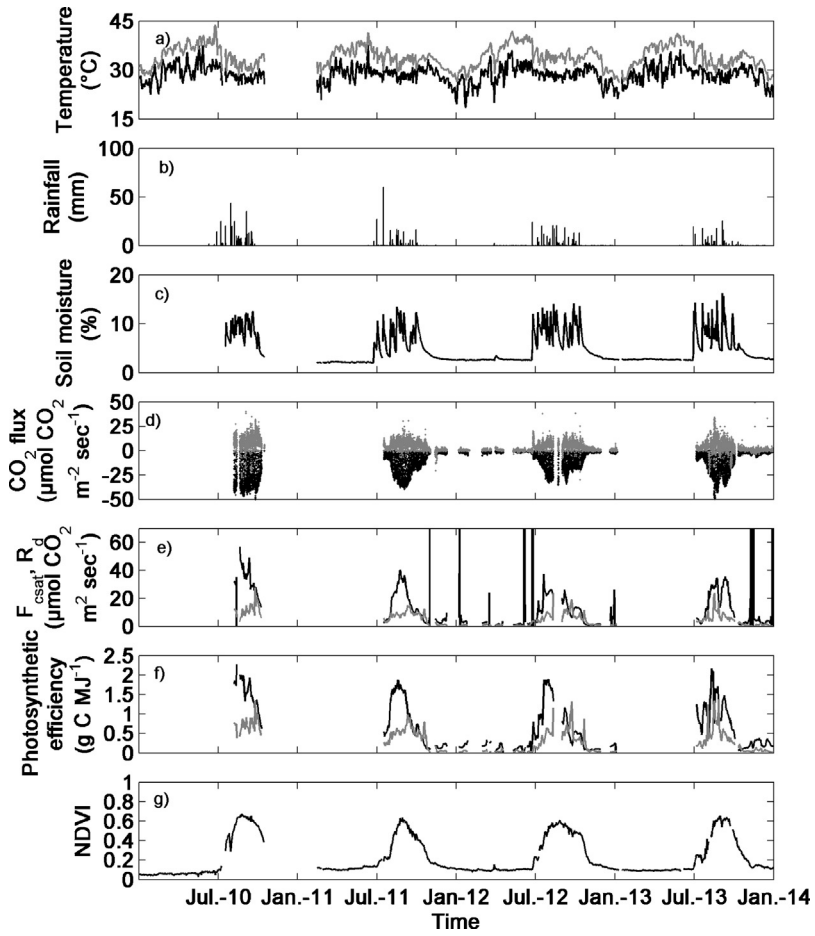

Fig. 3. Time series of the measured CO_2 fluxes and environmental variables 2010–2013. a) daily mean of air (black) and soil temperature (grey), b) daily sums of rainfall, c) daily mean of soil moisture at 5 cm depth, d) gross primary productivity (GPP) (black) and ecosystem respiration (R_{eco}) (grey), e) daily values of saturation level of GPP (F_{csat}) (black) and dark respiration (R_d) (grey), f) the light use efficiency (ε) (black) and the quantum efficiency (α) (grey), and g) the normalized difference vegetation index (NDVI).

correlated with air temperature ($r = 0.93$), rainfall ($r = -0.89$), leaf area index ($r = -0.87$), start and end of rainy season ($r = 0.86$ for both), and biomass ($r = -0.80$). Significant correlations were seen for the NEE budgets against biomass ($r = -0.98$) and growing season peak value of NDVI ($r = -0.96$), and strong non-significant correlations were seen against and length of rainy season ($r = 0.84$) and leaf area index ($r = 0.82$). The low number of statistically significant correlations between measured variables and the flux budgets were caused by the few number of years measured ($n = 4$; Table 3).

The uncertainty analysis of random and systematic errors of the flux measurements resulted in average total accumulated errors of 14.7%, 4.2% and 11.2%, for NEE, GPP, and R_{eco}, respectively. E_{rand} was 0.66%, E_{freq} was 2.4%, of the measured CO_2 fluxes. The average E_{gap} were 6.2%, 2.2% and 8.8%, and the average E_{filt} were 13.2%, 2.7% and 6.0% for NEE, GPP and R_{eco}, respectively.

Table 3
Annual values of carbon fluxes, hydroclimatic and environmental variables. The leaf area index (LAI) estimates are peak values from the MODIS LAI (MOD15A2) product. The normalised difference vegetation index (NDVI) is based on daily in-situ measurements (Section 2.3). The rainy season starts and ends at the first and final day of year with rain. DOY is day of year, NEE is net ecosystem exchange, GPP is gross primary productivity, and R_{eco} is ecosystem respiration.

Year	2010	2011	2012	2013
Air temperature (°C)	27.9	28.3	28.1	28.7
Rainfall (mm)	650.3	486.0	606.0	355.2
Species count	36	35	32	30
Peak LAI	2.1	1.7	1.4	1.4
Peak NDVI	0.68	0.64	0.61	0.65
Annual sum NDVI	75	76	84	77
Rainy season sum NDVI	41	40	53	48
Rainy season start (DOY)	174	176	176	182
Rainy season end (DOY)	267	278	289	291
Rainy season length (days)	93	102	113	109
Peak dry weight above ground herbaceous Biomass ($g\,C\,m^{-2}$)	236	111	103	133
Peak dry weight below ground herbaceous Biomass ($g\,C\,m^{-2}$)	142	67	62	80
Peak dry weight total herbaceous Biomass ($g\,C\,m^{-2}$)	378	178	165	213
NEE budgets ($g\,C\,m^{-2}$)	-336 ± 29	-247 ± 46	-227 ± 22	-273 ± 20
GPP budgets ($g\,C\,m^{-2}$)	-1263 ± 45	-1035 ± 47	-1072 ± 51	-935 ± 34
R_{eco} budgets ($g\,C\,m^{-2}$)	852 ± 100	776 ± 116	826 ± 100	637 ± 187

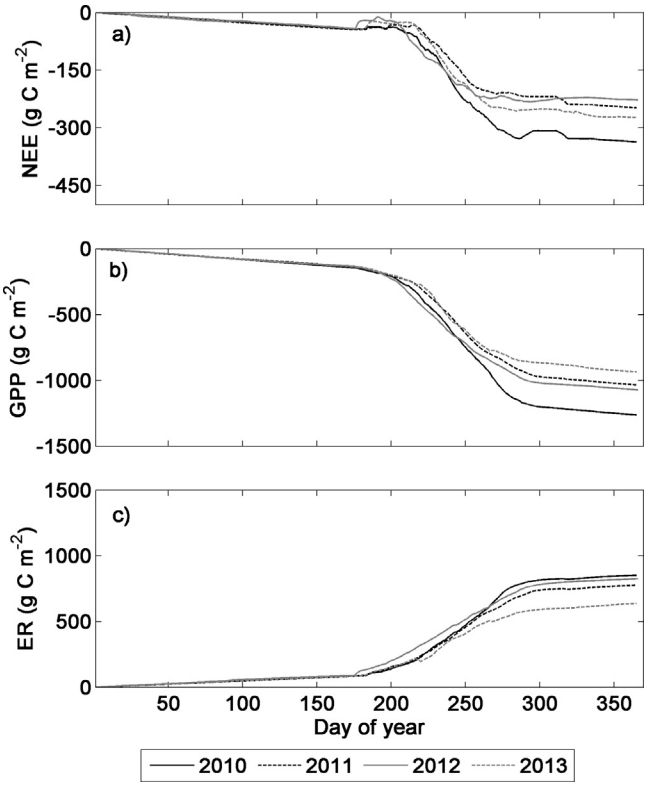

Fig. 4. Cumulative plots for the years 2010–2013 for a) net ecosystem exchange (NEE) (g C m^{-2}), b) gross primary productivity (GPP) (g C m^{-2}), and c) ecosystem respiration (R_{eco}) (g C m^{-2}).

4. Discussion

4.1. Seasonal dynamics in CO_2 fluxes

Similar seasonal dynamics in CO_2 flux for semi-arid areas with pronounced rainy seasons have previously been reported (e.g. Veenendaal et al., 2004; Xu and Baldocchi, 2004; Brümmer et al., 2008). But the measured fluxes at the peak of the rainy season were very high compared to other African semi-arid sites (Verhoef et al., 1996; Hanan et al., 1998; Veenendaal et al., 2004; Brümmer et al., 2008; Kutsch et al., 2008; Boulain et al., 2009; Merbold et al., 2009; Sjöström et al., 2009). Instead, the NEE reported here are similar to fluxes reported for humid tropical grassland, tropical C4 wetland plants, and fertilized and high precipitation temperate C4 grassland species (Kim et al, 1992; Dugas et al., 1999; Morison et al., 2000; Merbold et al., 2009; Saunders et al., 2012). The very strong correlation between total herbaceous biomass and the annual NEE budgets still indicates reasonable flux budgets. The discrepancies seen could be caused by: (1) grazing of animals; (2) tree C uptake included in the EC budgets; (3) spatial variability in the area affecting the plot based biomass estimate; (4) biomass harvesting being done every ten day and possibly missing the actual peak; and (5) uncertainties in the EC flux budgets. For example, the discrepancy for 2010 could possibly be explained by a relatively late start of the EC measurements in the rainy season.We have further evaluated the quality of the flux measurements; energy budget closures were reasonable, a cospectrum analysis indicated no overestimation of the LI-7500 sensor, and a comparison campaign at the site between the open path LI-7500 sensor and a closed path system indicated similar fluxes (preliminary data).

Possible explanations for the high CO_2 fluxes are a high fraction of C4 species, alleviated water stress conditions, and a strong grazing pressure that results in compensatory growth and fertilization effects. In areas of broadly similar climate, several factors can influences the fluxes, such as solar irradiance, species composition, anthropogenic factors, cultivation, fire sequences, disturbances, soil type, nutrient variability and age of the vegetation (Semmartin and Oesterheld, 1996; Rockström and de Rouw, 1997; Tagesson et al., 2009; Hutley and Beringer, 2011; Vourlitis and Ribeiro da Rocha, 2011).

4.2. Environmental controls on CO_2 fluxes

None of the environmental variables could be shown to control the half-hourly night-time NEE. For many biomes, it has been shown that temperature has a strong influence on R_{eco} and it is a strong factor governing the metabolism of plants and decomposers (e.g. Lloyd and Taylor, 1994; Tagesson and Lindroth, 2007). For this reason, temperature response curves are commonly applied for partitioning of NEE to GPP and R_{eco} (Reichstein et al., 2005). However, in the semi-arid tropics it is almost always warm enough for physiological activity and temperature is not a limiting factor (e.g. Hanan et al., 1998, 2011; Archibald et al., 2009), which explains the limited night-time NEE variability. The lack of relationship at our study site thereby confirm the findings by Archibald et al. (2009) that care should be taken before applying temperature response curves for hot dry semi-arid savanna ecosystems.

Gross primary productivity increases in the morning following the change in incoming radiation. But as the radiation and temperature increases, stomata closes in order to avoid water losses at the peak of the day (Lasslop et al., 2010); GPP thereby peaks before noon and have slightly lower values in the afternoon. The seasonal dynamics in GPP were as well strongly affected by soil moisture and VPD. It has also previously been shown that photosynthesis and productivity in semi-arid savanna ecosystems are highly governed by water availability, and VPD additionally governs the air's ability to extract water from the plants (Moncrieff et al., 1997b; Kutsch et al., 2008; Merbold et al., 2009).

The main factor determining the seasonal variation in all CO_2 exchange fluxes (NEE, GPP and R_{eco}) was NDVI, i.e. the phenology of the vegetation, indicating the importance of vegetation parameters for the CO_2 exchange fluxes (Moncrieff et al., 1997b). The vegetation phenology governs the leaf development, and a high leaf area gives high light absorption capacity, and thus a high photosynthetic CO_2 uptake. The NDVI of Dahra was high in relation to NDVI of other EC sites in the Sahel, possibly explaining the large CO_2 fluxes seen at the site (Ardö et al., 2008; Boulain et al., 2009; Merbold et al., 2009). The NDVI is also an indicator of biomass quality and availability, governing both autotrophic and heterotrophic respiration, explaining the strong impact on R_{eco}. Ecosystem respiration was also related with GPP, confirming the strong influence of vegetation productivity on R_{eco} (e.g. Janssens et al., 2001). The litter decay rates differ between plant functional types, with high rates of decomposition for grasses and low rates for shrubs and forbs (Meentemeyer, 1978). There are possible changes in plant functional types across the Sahel in the future, with a stronger dominance of shrubs and trees (Sitch et al., 2008), which would alter the CO_2 flux for the region.

4.3. Light use efficiency

The peak ε at Dahra was 2.27 g C MJ^{-1} APAR, i.e. substantially higher than the peak ε values in the biome parameter look-up table used in the calculation of GPP in the MOD17A2 algorithm for savannas (1.21 g C MJ^{-1} APAR) (Zhao and Running, 2010). It has

been shown that ε can vary substantially both within and between vegetation types (e.g. Lagergren et al., 2005; Garbulsky et al., 2010; Tagesson et al., 2012a; Sjöström et al., 2013). For savannas, peak ε is varying from 0.33 g C MJ^{-1}APAR to 3.50 g C MJ^{-1}APAR (Sjöström et al., 2013 and references therein). Given the high CO_2 accumulation rates at Dahra, it seems odd that peak ε is in the upper middle part of this range. However, by comparison to the fraction of PAR absorbed by the vegetation reported by Sjöström et al. (2013) (peak values ~0.4), the fraction of PAR absorbed by the vegetation was ~2 times higher in Dahra (peak values ~0.8).

At the Dahra site, it was shown that NDVI was most strongly coupled to ε variability. It has also previously been shown that vegetation parameters have important influences on ε, for example by varying vegetation type and C3/C4 species ratio (Merbold et al., 2009; Sjöström et al., 2013). Generally, ecosystems dominated by trees have lower ε than ecosystems dominated by grasses (Garbulsky et al., 2010), possibly explaining the relatively high ε values at Dahra. Dynamics in ε was also affected by water availability (soil moisture and VPD), again confirming the strong link between water availability and vegetation productivity for semi-arid savanna ecosystems (Moncrieff et al., 1997b; Kutsch et al., 2008; Merbold et al., 2009). It has also previously been shown that rainfall governs both global and continental scale spatial variation in ε (Garbulsky et al., 2010; Sjöström et al., 2013). To avoid water losses, vegetation closes their stomata as radiation and temperature increases (Lasslop et al., 2010), explaining the influence by PAR and air temperature on the seasonal dynamics on ε as well. Generally, when modeling GPP using the LUE approach variable FAPAR is applied to the model whereas ε is assigned to a vegetation type (e.g. Gower et al., 1999; Tagesson et al., 2012a), and very few studies couple ε with biophysical variables (Garbulsky et al., 2010). Our results demonstrate that this variability in ε may be hard to spatially and temporally describe with broad land cover class values, and without consideration of variability in biophysical variables.

4.4. The annual C flux budgets

The measured fluxes at the Dahra site was very high at the peak of the growing season, but since the growing season was short, the annual budgets were not larger than at other semi-arid sites (Chen et al., 2003; Brümmer et al., 2008; Archibald et al., 2009; Ciais et al., 2011). Ciais et al. (2011) reported a median NEE budget of 230 g C m^{-2} for many in situ and model studies, which is very similar to the NEE budgets of Dahra (Table 3). Chen et al. (2003) reported an annual GPP budget of 2080 g C m^{-2}, and a R_{eco} budget of 1700 g C m^{-2} for a tropical savanna in northern Australia, i.e. higher than at Dahra. Veenendaal et al. (2004) measured a *C. mopane* savanna woodland in Botswana, which was almost in C balance (annual NEE budget of ~−12 g CO_2 m^{-2}), but with GPP and R_{eco} budgets of ~1300 g C m^{-2}. It has previously been shown that inter-annual variation in C budgets for semi-arid savanna ecosystems is strongly affected by water availability and rainfall distribution (Moncrieff et al., 1997b; Brümmer et al., 2008). We can confirm this observation in that both the GPP and R_{eco} budgets were strongly affected by rainfall, and start of rainy season. Both R_{eco} and GPP was negatively affected by temperature, most likely explained by the negative feedback temperature has on the water availability for the ecosystem. The only climatic factor with a strong influence on the NEE was the length of the rainy season. Global circulation models project a decrease in rainfall, an increase in temperature for the western Sahel region and a reduction in growing season length (Sarr, 2012; Roehrig et al., 2013). This may thus affect the productivity and the sink function of the ecosystems in the Sahel region negatively in the future.

Acknowledgements

This paper was written within the frame of the project entitled Earth Observation based Vegetation productivity and Land Degradation Trends in Global Drylands. The project was funded by the Danish Council for Independent Research (DFF) Sapere Aude programme. Faculty of Science, Lund University supported the measurements with an infrastructure grant. Ardö was supported by a grant from the Swedish National Space Board. We are very grateful to the Institut des Sciences de l'Environnement at the Université Cheikh Anta de Dakar and to the Institut Sénégalais de Recherche Agricole for all logistic, administrative and technical support. Thanks also to our guards who provided night and day surveillance of the study site.

Appendix A. Error analysis

Error analysis

When calculating CO_2 balances for longer periods, errors associated with the half-hourly measurements affect the long term budgets. Random error (E_{rand}) was estimated following the method by Finkelstein and Sims (2001), where variance of the covariance between CO_2 concentration and vertical wind speed gives an estimate of the sampling error in the EC measurements. The E_{rand} is typically low for long time series, such as annual budgets, whereas systematic errors may be more severe (Aurela et al., 2002). The systematic errors were estimated following the method by Aurela et al. (2002):

Errors from the gap filling (E_{gf}) using the light response function were estimated by calculating the fluxes with different length of the moving window when fitting of the parameters in Eqs. (3) and (5) (3–13 day long moving windows). The E_{gf} associated with the gap filling of the gaps longer than 3 days were estimated from the uncertainty in 100 CO_2 flux estimates from the regression trees.

Filtering of fluxes measured during low turbulent conditions during night-time is considered one of the largest sources of uncertainty in long term budgets of CO_2 fluxes and the size of the annual budgets greatly depends on the selection of threshold for the filtering criteria (e.g. Goulden et al., 1996). We assessed the errors associated with the filtering (E_{filt}) by calculating annul balances by using different threshold criterias for the overall quality flags (threshold values: 1–6).

A commonly acknowledged systematic source of error is the insufficient coverage of high frequencies (E_{freq}) contributing to the fluxes. An uncertainty of 30% for the correction procedure of the loss of high frequencies were assumed following Aurela et al. (2002). The error analysis does not include all error sources, but it provides an estimate of the main uncertainties in the flux measurements.

References

Archibald, S.A., Kirton, A., van der Merwe, M.R., Scholes, R.J., Williams, C.A., Hanan, N., 2009. Drivers of inter-annual variability in net ecosystem exchange in a semi-arid savanna ecosystem, South Africa. Biogesciences 6, 251–266.

Ardö, J., Mölder, M., El-Tahir, B., Elkhidir, H., 2008. Seasonal variation of carbon fluxes in a sparse savanna in semi arid Sudan. Carbon Balance Manage. 3, 7.

Aurela, M., Laurila, T., Tuovinen, J.P., 2002. Annual CO_2 balance of a subarctic fen in northern Europe: importance of the wintertime efflux. J. Geophys. Res. 107, 4607.

Boulain, N., Cappelaere, B., Ramier, D., Issoufou, H.B.A., Halilou, O., Seghieri, J., Guillemin, F., Oï, M., Gignoux, J., Timouk, F., 2009. Towards an understanding of coupled physical and biological processes in the cultivated Sahel –. J. Hydrol. 375, 190–203.

Brümmer, C., Falk, U., Papen, H., Szarzynski, J., Wassmann, R., Brüggemann, N., 2008. Diurnal, seasonal, and interannual variation in carbon dioxide and energy exchange in shrub savanna in Burkina Faso (West Africa). J. Geophys. Res. 113, G02030.

Chapin, F.S., Matson, P.A., Mooney, H.A., 2002. Principles of Terrestrial Ecosystem Ecology. Springer, New York.
Chen, X., Hutley, L., Eamus, D., 2003. Carbon balance of a tropical savanna of northern Australia. Oecologia 137, 405–416.
Ciais, P., Bombelli, A., Williams, M., Piao, S.L., Chave, J., Ryan, C.M., Henry, M., Brender, P., Valentini, R., 2011. The carbon balance of Africa: synthesis of recent research studies. Philos. Trans. R. Soc. A: Math. Phys. Eng. Sci. 369, 2038–2057.
De'ath, G., Fabricius, K.E., 2000. Classification and regression trees: a powerful yet simple technique for ecological data analysis. Ecology 81, 3178–3192.
Donohue, R.J., Roderick, M.L., McVicar, T.R., Farquhar, G.D., 2013. Impact of CO_2 fertilization on maximum foliage cover across the globe's warm, arid environments. Geophys. Res. Lett. 40, 3031–3035.
Drolet, G.G., Middleton, E.M., Huemmrich, K.F., Hall, F.G., Amiro, B.D., Barr, A.G., Black, T.A., McCaughey, J.H., Margolis, H.A., 2008. Regional mapping of gross light-use efficiency using MODIS spectral indices. Remote Sens. Environ. 112, 3064–3078.
Dugas, W.A., Heuer, M.L., Mayeux, H.S., 1999. Carbon dioxide fluxes over bermudagrass native prairie, and sorghum. Agric. For. Meteorol. 93, 121–139.
Falge, E., Baldocchi, D., Olson, R., Anthoni, P., Aubinet, M., Bernhofer, C., Burba, G., Ceulemans, R., Clement, R., Dolman, H., Granier, A., Gross, P., Grunwald, T., Hollinger, D., Jensen, N.O., Katul, G., Keronen, P., Kowalski, A., Lai, C.T., Law, B.E., Meyers, T., Moncrieff, J., Moors, E., Munger, J.W., Pilegaard, K., Rannik, U., Rebmann, C., Suyker, A., Tenhunen, J., Tu, K., Verma, S., Vesala, T., Wilson, K., Wofsy, S., 2001. Gap filling strategies for defensible annual sums of net ecosystem exchange. Agric. For. Meteorol. 107, 43–69.
Fan, S.M., Wofsy, S.C., Bakwin, P.S., Jacob, D.J., Fitzjarrald, D.R., 1990. Atmosphere–biosphere exchange of CO_2 and O_3 in the Central Amazon Forest. J. Geophys. Res. 95, 16851–16864.
Fensholt, R., Sandholt, I., Rasmussen, M.S., 2004. Evaluation of MODIS LAI, fAPAR and the relation between fAPAR and NDVI in a semi-arid environment using in situ measurements. Remote Sens. Environ. 91, 490–507.
Finkelstein, P.L., Sims, P.F., 2001. Sampling error in eddy correlation flux measurements. J. Geophys. Res. 106, 3503–3509.
Foken, T., Gøckede, M., Mauder, M., Mahrt, L., Amiro, B., Munger, W., 2004. Post-field data quality control. In: Lee, J.A., Massman, W., Law, B. (Eds.), Handbook of Micrometerology – A guidebook for Surface Flux Measurement and Analysis. Kluwer Academic Publishers, London.
Friborg, T., Boegh, E., Soegaard, H., 1997. Carbon dioxide flux, transpiration and light response of millet in the Sahel. J. Hydrol. 188–189, 633–650.
Garbulsky, M.F., Peñuelas, J., Papale, D., Ardö, J., Goulden, M.L., Kiely, G., Richardson, A.D., Rotenberg, E., Veenendaal, E.M., Filella, I., 2010. Patterns and controls of the variability of radiation use efficiency and primary productivity across terrestrial ecosystems. Global Ecol. Biogeogr. 19, 253–267.
Goetz, S.J., Prince, S.D., 1996. Remote sensing of net primary production in boreal forest stands. Agric. For. Meteorol. 78, 149–179.
Goulden, M.L., Munger, J.W., Fan, S.-M., Daube, B.C., Wofsy, S.C., 1996. Measurements of carbon sequestration by long-term eddy covariance: methods and a critical evaluation of accuracy. Global Change Biol. 2, 169–183.
Gower, S.T., Kucharik, C.J., Norman, J.M., 1999. Direct and indirect estimation of leaf area index, fAPAR, and net primary production of terrestrial ecosystems – a real or imaginary problem? Remote Sens. Environ. 70, 29–51.
Hanan, N., Kabat, P., Dolman, J., Elbers, J.A.N., 1998. Photosynthesis and carbon balance of a Sahelian fallow savanna. Global Change Biol. 4, 523–538.
Hanan, N., Boulain, N., Williams, C., Scholes, R., Archibald, S., 2011. Functional convergence in ecosystem carbon exchange in adjacent savanna vegetation types of the Kruger National Park, South Africa. In: Hill, M.J., Hanan, N. (Eds.), Ecosystem Function in Savannas. CRC Press, Boca Raton, pp. 57–76.
Hickler, T., Eklundh, L., Seaquist, J.W., Smith, B., Ardo, J., Olsson, L., Sykes, M.T., Sjostrom, M., 2005. Precipitation controls Sahel greening trend. Geophys. Res. Lett. 32.
Hutley, L.B., Beringer, J., 2011. Disturbance and climatic drivers of carbon dynamics of a North Australian tropical savanna. In: Hill, M.J., Hanan, N. (Eds.), Ecosystem Function in Savannas. CRC Press, Boca Raton, pp. 57–76.
Janssens, I.A., Lankreijer, H., Matteucci, G., Kowalski, A.S., Buchmann, N., Epron, D., Pilegaard, K., Kutsch, W., Longdoz, B., Grünwald, T., Montagnani, L., Dore, S., Rebmann, C., Moors, E.J., Grelle, A., Rannik, Ü., Morgenstern, K., Oltchev, S., Clement, R., GuÐmundsson, J., Minerbi, S., Berbigier, P., Ibrom, A., Moncrieff, J., Aubinet, M., Bernhofer, C., Jensen, N.O., Vesala, T., Granier, A., Schulze, E.D., Lindroth, A., Dolman, A.J., Jarvis, P.G., Ceulemans, R., Valentini, R., 2001. Productivity overshadows temperature in determining soil and ecosystem respiration across European forests. Global Change Biol. 7, 269–278.
Kim, J., Verma, S.B., Clement, R.J., 1992. Carbon dioxide budget in temperate grassland ecosystem. J. Geophys. Res. 97, 6057–6063.
Kutsch, W.L., Hanan, N., Scholes, B., McHugh, I., Kubheka, W., Eckhardt, H., Williams, C., 2008. Response of carbon fluxes to water relations in a savanna ecosystem in South Africa. Biogeosciences 5, 1797–1808.
Lagergren, F., Eklundh, L., Grelle, A., Lundblad, M., Molder, M., Lankreijer, H., Lindroth, A., 2005. Net primary production and light use efficiency in a mixed coniferous forest in Sweden. Plant Cell Environ. 28, 412–423.
Lasslop, G., Reichstein, M., Papale, D., 2010. Separation of net ecosystem exchange into assimilation and respiration using a light response curve approach: critical issues and global evaluation. Global Change Biol 16, 187–209.
LI-COR Biosciences, 2012. EDDYPRO Eddy Covariance Software Version 4.0 User's Guide & Reference. LI-COR Inc., Lincoln.
Lloyd, J., Taylor, J.A., 1994. On the temperature dependence of soil respiration. Funct. Ecol. 8, 315–323.
Mbow, C., Fensholt, R., Rasmussen, K., Diop, D., 2013. Can vegetation productivity be derived from greenness in a semi-arid environment? Evidence from ground-based measurements. J. Arid Environ. 97, 56–65.
Meentemeyer, V., 1978. Macroclimate and lignin control of litter decomposition rates. Ecology 59, 465–472.
Merbold, L., Ardö, J., Arneth, A., Scholes, R.J., Nouvellon, Y., de Grandcourt, A., Archibald, S., Bonnefond, J.M., Boulain, N., Brueggemann, N., Bruemmer, C., Cappelaere, B., Ceschia, E., El-Khidir, H.A.M., El-Tahir, B.A., Falk, U., Lloyd, J., Kergoat, L., Le Dantec, V., Mougin, E., Muchinda, M., Mukelabai, M.M., Ramier, D., Roupsard, O., Timouk, F., Veenendaal, E.M., Kutsch, W.L., 2009. Precipitation as driver of carbon fluxes in 11 African ecosystems. Biogeosciences 6, 1027–1041.
Moncrieff, J.B., Massheder, J.M., de Bruin, H., Elbers, J., Friborg, T., Heusinkveld, B., Kabat, P., Scott, S., Soegaard, H., Verhoef, A., 1997a. A system to measure surface fluxes of momentum, sensible heat, water vapour and carbon dioxide. J. Hydrol. 188–189, 589–611.
Moncrieff, J.B., Monteny, B., Verhoef, A., Friborg, T., Elbers, J., Kabat, P., de Bruin, H., Soegaard, H., Jarvis, P.G., Taupin, J.D., 1997b. Spatial and temporal variations in net carbon flux during HAPEX-Sahel. J. Hydrol. 188–189, 563–588.
Moncrieff, J.B., Clement, R., Finnigan, J., Meyers, T., 2004. Averaging, detrending and filtering of eddy covariance time series. In: Lee, X., Massman, W.J., Law, B.E. (Eds.), Handbook of Micrometeorology: A Guide for Surface Flux Measurements. Kluwer Academic, Dordrecht, pp. 7–31.
Monteith, J.L., 1972. Solar radiation and productivity in tropical ecosystems. J. Appl. Ecol. 9, 747–766.
Monteith, J.L., 1977. Climate and the efficiency of crop production in Britain. Philos. Trans. R. Soc. B. 281, 277–294.
Morison, J.I.L., Piedade, M.T.F., Müller, E., Long, S.P., Junk, W.J., Jones, M.B., 2000. Very high productivity of the C4 aquatic grass *Echinochloa polystachya* in the Amazon floodplain confirmed by net ecosystem CO_2 flux measurements. Oecologia 125, 400–411.
OECD, 2009. Chapter 15. Vulnerability in the Sahelian Zone. In: Bossard, L. (Ed.), West African Studies: Regional Atlas on West Africa. OECD Publishing, Paris, pp. 269–284.
Poulter, B., Frank, D., Ciais, P., Myneni, R.B., Andela, N., Bi, J., Broquet, G., Canadell, J. G., Chevallier, F., Liu, Y.Y., Running, S.W., Sitch, S., van der Werf, G.R., 2014. Contribution of semi-arid ecosystems to interannual variability of the global carbon cycle. Nature 509, 600–603.
Rasmussen, M.O., Göttsche, F.M., Diop, D., Mbow, C., Olesen, F.S., Fensholt, R., Sandholt, I., 2011. Tree survey and allometric models for tiger bush in northern Senegal and comparison with tree parameters derived from high resolution satellite data. Int. J. Appl. Earth Obs. Geoinf. 13, 517–527.
Reichstein, M., Falge, E., Baldocchi, D., Papale, D., Aubinet, M., Berbigier, P., Bernhofer, C., Buchmann, N., Gilmanov, T., Granier, A., Grunwald, T., Havrankova, K., Ilvesniemi, H., Janous, D., Knohl, A., Laurila, T., Lohila, A., Loustau, D., Matteucci, G., Meyers, T., Miglietta, F., Ourcival, J.-M., Pumpanen, J., Rambal, S., Rotenberg, E., Sanz, M., Tenhunen, J., Seufert, G., Vaccari, F., Vesala, T., Yakir, D., Valentini, R., 2005. On the separation of net ecosystem exchange into assimilation and ecosystem respiration: review and improved algorithm. Global Change Biol. 11, 1424–1439.
Rockström, J., de Rouw, A., 1997. Water, nutrients and slope position in on-farm pearl millet cultivation in the Sahel. Plant Soil 195, 311–327.
Roehrig, R., Bouniol, D., Guichard, F., Hourdin, F., Redelsperger, J.L., 2013. The present and future of the West African monsoon: a process-oriented assessment of CMIP5 simulations along the AMMA transect. J. Clim. 26, 6471–6505.
Sarr, B., 2012. Present and future climate change in the semi-arid region of West Africa: a crucial input for practical adaptation in agriculture. Atmos. Sci. Lett. 13, 108–112.
Saunders, M.J., Kansiime, F., Jones, M.B., 2012. Agricultural encroachment: implications for carbon sequestration in tropical African wetlands. Global Change Biol. 18, 1312–1321.
Schlesinger, W.H., 1997. Biogeochemistry – An Analysis of Global Change, 2nd ed. Academic Press, Harcourt Brace & Co. Publishers, London, UK.
Semmartin, M., Oesterheld, M., 1996. Effect of grazing pattern on primary productivity. Oikos 75, 431–436.
Sitch, S., Huntingford, C., Gedney, N., Levy, P.E., Lomas, M., Piao, S.L., Betts, R., Ciais, P., Cox, P., Friedlingstein, P., Jones, C.D., Prentice, I.C., Woodward, F.I., 2008. Evaluation of the terrestrial carbon cycle, future plant geography and climate–carbon cycle feedbacks using five dynamic global vegetation models (DGVMs). Global Change Biol. 14, 2015–2039.
Sjöström, M., Ardö, J., Eklundh, L., El-Tahir, B.A., El-Khidir, H.A.M., Hellström, M., Pilesjö, P., Seaquist, J., 2009. Evaluation of satellite based indices for gross primary production estimates in a sparse savanna in the Sudan. Biogeosciences 6, 129–138.
Sjöström, M., Zhao, M., Archibald, S., Arneth, A., Cappelaere, B., Falk, U., de Grandcourt, A., Hanan, N., Kergoat, L., Kutsch, W., Merbold, L., Mougin, E., Nickless, A., Nouvellon, Y., Scholes, R.J., Veenendaal, E.M., Ardö, J., 2013. Evaluation of MODIS gross primary productivity for Africa using eddy covariance data. Remote Sens. Environ. 131, 275–286.
Tagesson, T., Lindroth, A., 2007. High soil carbon efflux rates in several ecosystems in southern Sweden. Boreal Environ. Res. 12, 65–80.
Tagesson, T., Smith, B., Löfgren, A., Rammig, A., Eklundh, L., Lindroth, A., 2009. Estimating net primary production of Swedish forest landscapes by combining mechanistic modeling and remote sensing. Ambio 38, 316–324.
Tagesson, T., Mastepanov, M., Tamstorf, M.P., Eklundh, L., Schubert, P., Ekberg, A., Sigsgaard, C., Christensen, T.R., Ström, L., 2012a. High-resolution satellite data

reveal an increase in peak growing season gross primary production in a high-Arctic wet tundra ecosystem 1992–2008. Int. J. Appl. Earth Obs. Geoinf. 18, 407–416.
Tagesson, T., Mölder, M., Mastepanov, M., Sigsgaard, C., Tamstorf, M.P., Lund, M., Falk, J.M., Lindroth, A., Christensen, T.R., Ström, L., 2012b. Land-atmosphere exchange of methane from soil thawing to soil freezing in a high-Arctic wet tundra ecosystem. Global Change Biol. 18, 1928–1940.
Tagesson, T., Fensholt, R., Guiro, I., Rasmussen, M.O., Huber, S., Mbow, C., Garcia, M., Horion, S., Sandholt, I., Holm-Rasmussen, B., Göttsche, F.M., Ridler, M.-E., Olén, N., Olsen, J.L., Ehammer, A., Madsen, M., Olesen, F.S., Ardö, J., 2015. Ecosystem properties of semi-arid savanna grassland in West Africa and its relationship to environmental variability. Global Change Biol. 21, 250–264.
Veenendaal, E.M., Kolle, O., Lloyd, J., 2004. Seasonal variation in energy fluxes and carbon dioxide exchange for a broadleaved semi-arid savanna (Mopane woodland) in Southern Africa. Global Change Biol. 10, 318–328.
Verhoef, A., Allen, S.J., De Bruin, H.A.R., Jacobs, C.M.J., Heusinkveld, B.G., 1996. Fluxes of carbon dioxide and water vapour from a Sahelian savanna. Agric. For. Meteorol. 80, 231–248.
Vickers, D., Mahrt, L., 1997. Quality control and flux sampling problems for tower and aircraft data. J. Atmos. Ocean. Tech. 14, 152–526.
Vourlitis, G., Ribeiro da Rocha, H., 2011. Flux dynamics in the Cerrado and Cerrado-forest transition of Brazil. In: Hill, M.J., Hanan, N. (Eds.), Ecosystem Function in Savannas. CRC Press, Boca Raton, pp. 57–76.
Webb, E.K., Pearman, G.I., Leuning, R., 1980. Correction of the flux measurements for density effects due to heat and water vapour transfer. Q. J. R. Meteor. Soc. 106, 85–100.
Wilczak, J.M., Oncley, S.P., Stage, S.A., 2001. Sonic anemometer tilt correction algorithms. Boundary Layer Meteorol. 99, 127–150.
Wilsey, B., Wayne, P.H., 2006. Aboveground productivity and root–shoot allocation differ between native and introduced grass species. Oecologia 150, 300–309.
Xu, L., Baldocchi, D., 2004. Seasonal variation in carbon dioxide exchange over a Mediterranean annual grassland in California. Agric. For. Meteorol. 123, 79–96.
Zhao, M., Running, S.W., 2010. Drought-induced reduction in global terrestrial net primary production from 2000 through 2009. Science 329, 940–943.